CORRELATION-STATISTICS-BASED SIMULATOR OF PERTURBED PHASES TRIGGERED BY THE IONOSPHERIC IRREGULARITIES FOR HF RADAR SYSTEMS

Yongpeng Zhu[†] *Yinsheng Wei*[†] *Peng Tong*[†]

[†] School of Electronics and Information Engineering, Harbin Institute of Technology, Harbin, China
weiys@hit.edu.cn

ABSTRACT

It transpires that the irregularity in the structure of the ionospheric plasma plays a significant role on the ionospherically-propagated HF signals. In this paper, special attention has been paid to derive a simulator that can explicate the perturbed phase influence imposed by the ionosphere irregularities. This has been achieved by studying the space-time correlation as well as statistics of the perturbed phases so that the problem of perturbed phase simulation is recast as generating particular time series satisfying specific power spectrum and statistical distribution. Eventually, three scenarios corresponding to different irregularity fluctuation conditions are considered to verify the effectiveness of the proposed simulator. It is shown numerically that the obtained perturbed phases can agree well with the theoretical assumptions.

Index Terms— HF radar, ionospheric irregularities, multiple phase-screen method, zero memory nonlinear transform

1. INTRODUCTION

It is well known that the ionosphere constitutes the major reflection medium to permit the target detection over the horizon in the HF radar systems, such as the HF skywave radar and hybrid sky-surface wave radar [1]-[3]. However, the involvement of ionosphere non-uniform random medium also enhances the spectral complexity of the ocean echoes and therefore degrades the performance of target discrimination and clutter suppression.

The ionospheric irregularities captured as the density structure within the ionospheric plasma would cause the additional phase perturbations deteriorating the signal coherence during transit, which places a lower bound on the precision of target angular and Doppler information, and to a lesser extent range information. Intuitively, an understanding of perturbation characteristics would be essential for improving the radar detection performance. Allowing for the past research, several insightful results have been obtained and thus improved this investigation to a large extent. Based upon the approximation of geometric optics, Coleman [4] modelled the ionosphere as a combination of quiet and disturbed ionospheric conditions so that the scattered wave field expressed by a linear integral of the refractive index could be divided into two components representing the background ionosphere and irregularity contributions. Based on this assumption, the phase perturbation was evaluated by a first order Taylor series to the total phase accrued during the propagation according to the Fermat's principle [5]. Afterwards the geometric optics method was further developed by Kiang [6] with the introduction of phase screens interpolated into the free space to explain the random phase fluctuation. And the multiple phase-screen method for the oblique incidence case was proposed by Wagen in [7]. Besides, to consider the diffractive effects, Rytov [8] addressed this problem by expressing the scattered wave field as a complex value so as to capture the amplitude and phase effects in a straightforward way.

This work is supported by the National Natural Science Foundation of China under grant No.61471144.

In this paper, the space-time correlation and statistical distribution of perturbed phases are firstly studied in section 2. Based upon which, a simulator is afterwards derived to generate the specific time series to simulate the perturbed phases obeying specific power spectrum and statistical property. In section 3, the validity of the proposed method is verified by accommodating to several particular situations. Eventually, a brief summary is given in section 4.

2. ANALYSIS OF IONOSPHERIC PERTURBED PHASES IN SPACE-TIME CORRELATION AND STATISTICAL DISTRIBUTION

Herein, of particular interests are the perturbed phase influence imposed by the ionosphere irregularities. Given that such perturbation is varying both in space and time, the stochastic method appears to be a more appropriate alternative. In the following, we will study the space-time correlation and statistical property of the ionosphere perturbed phases through theoretical derivation and simulation tests.

2.1. Autocorrelation Analysis of the Perturbed Phases in Space and Time

In general, we consider a Cartesian system of coordinates, with x east, y north and z vertical. Following [4],[9], the total

978-1-4799-9988-0/16/$31.00 ©2016 IEEE

ionosphere electron density n is reckoned as the combination of the quiescent background part n_0 and an irregular part n_1, namely $n = n_0 + n_1$. And the accumulated phase involving the irregularity influence can be evaluated by

$$\varphi_1(x,y) = -r_e\lambda \int_0^{z_t} \frac{n_1(x,y,z)}{\sqrt{1-z/z_t}} dz \tag{1}$$

Where r_e is the classical electron radius (2.8×10^{-15} m). λ is the radar wave length. z_t is the height corresponding to the reflection and $z_t = 0$ indicates the bottom of the ionosphere.

Invoking (1), the spatial autocorrelation over the horizon plane (x, y) can be estimated by the ensemble average of φ_1

$$\begin{aligned} &R_{\varphi_1}(X,Y) = \langle \varphi_1(x+X, y+Y)\, \varphi_1^*(x,y) \rangle \\ &= (r_e\lambda)^2 \int_0^{z_t}\int_0^{z_t} \frac{R_{n_1}\left(X,Y,z-z'\right)}{\sqrt{(1-z/z_t)(1-z'/z_t)}} dz dz' \end{aligned} \tag{2}$$

To calculate R_{φ_1}, we carry on the following derivation. Firstly, we let $u = \left(z - z'\right)/z_t$ and $v = \left(z + z'\right)/z_t$ so that the Jacobian determinant is $J(u,v) = \frac{\partial\left(z,z'\right)}{\partial(u,v)} = 1/\begin{vmatrix} \frac{\partial u}{\partial z} & \frac{\partial u}{\partial z'} \\ \frac{\partial v}{\partial z} & \frac{\partial v}{\partial z'} \end{vmatrix} = \frac{z_t^2}{2}$. Therefore, (2) can be reduced into

$$\begin{aligned} &R_{\varphi_1}(X,Y) = \tfrac{(r_e\lambda z_t)^2}{4} \\ &\cdot \int_{-1}^{1} R_{n_1}(X,Y,z_t u) \left[\int_{|u|}^{-|u|+2} \tfrac{2}{\sqrt{(2-v)^2-u^2}} dv\right] du \end{aligned} \tag{3}$$

Considering the φ_1-integral in the bracket of (3), notated as I_{φ_1}, the significant integrand contribution is merely along the strip $z \approx z'$ (i.e. $u \approx 0$) so that I_{φ_1} can be estimated by $I_{\varphi_1} = \int_{|u|}^{-|u|+2} \frac{2}{\sqrt{(2-v)^2-u^2}} dv \approx \lim_{u\to 0} I_{\varphi_1} = 2\ln\frac{4}{|u|} = 2(\ln 4 - \ln|u|) \approx 2\ln\frac{1}{|u|}$. In conjunction with the integrand result and the new definition of $Z = z_t u$, (3) is thus determined by

$$\begin{aligned} R_{\varphi_1}(X,Y) &= \frac{(r_e\lambda z_t)^2}{2} \int_{-1}^{1} R_{n_1}(X,Y,Z) \ln\frac{1}{|u|} du \\ &= \frac{z_t (r_e\lambda)^2}{2} \int_{-\infty}^{\infty} R_{n_1}(X,Y,Z) \ln\frac{z_t}{|Z|} \mu(z_t - |Z|) dZ \end{aligned} \tag{4}$$

Where $\mu(\cdot)$ is the unit step function. To distinguish the horizon wave number components corresponding to the perturbed phase spectrum from that of the propagating wave packet, $\boldsymbol{\kappa} = (\kappa_x, \kappa_y)$ is notated and the fluctuation phase spectrum can be yielded by two dimension Fourier transform on (X, Y)

$$\begin{aligned} S_{\varphi_1}(\kappa_x,\kappa_y) &= \frac{z_t (r_e\lambda)^2}{2} \int_{-\infty}^{\infty}\int_{-\infty}^{\infty}\int_{-\infty}^{\infty} R_{n_1}(X,Y,Z) \\ &\quad \cdot \ln\frac{z_t}{|Z|} \mu(z_t - |Z|)\, e^{-j\kappa_x X - j\kappa_y Y} dX dY dZ \\ &= \frac{(\lambda r_e z_t)^2}{2} \left\{ \frac{1}{2\pi} S_{n_1}(\kappa_x,\kappa_y,\kappa_z) \overset{\kappa_z}{*} \frac{2}{\kappa_z z_t} Si(\kappa_z z_t) \right\}\Bigg|_{\kappa_z=0} \\ &\approx \frac{(\lambda r_e z_t)^2}{2\pi} S_{n_1}(\kappa_x,\kappa_y,\kappa_z=0) \end{aligned} \tag{5}$$

Where κ_z-star indicates the convolution conducted on κ_z coordinate. As for S_{n_1} itself, the widely used spectrum following the Shkarofsky spectrum [10] is considered herein. Obviously, R_{φ_1} can be estimated by taking the inverse Fourier transform implementation of (5). And in lieu of a direct measurement of correlation, the complex signal amplitude containing the perturbed phases expressed by (6) is exploited to calculate the autocorrelation function

$$\begin{aligned} R_{A_c}(X,Y) &= \left\langle e^{-j\varphi_1(x,y) + j\varphi_1(x+X, y+Y)} \right\rangle \\ &= e^{R_{\varphi_1}(X,Y) - \left\langle \varphi_1^2 \right\rangle} \end{aligned} \tag{6}$$

From (4) to (5), (6) is reasonable to be simplified as

$$R_{A_c}(\rho_c) \approx 1 + \left\langle \varphi_1^2 \right\rangle \frac{\kappa_0^2 \rho_c^2}{\pi} \ln\frac{\kappa_0 \rho_c}{2} \tag{7}$$

In (7), $\left\langle \varphi_1^2 \right\rangle$ represents the mean-square phase fluctuation, κ_0 is the ionosphere outer scale parameter and ρ_c indicates the correlation scale in space. In what follows, the analysis of the temporal correlation is made by taking the inverse Fourier transform of the δ-function-inserted perturbation phase spectrum at $(X, Y) = 0$ in (8)

$$\begin{aligned} &R_{\varphi_1}(X=0, Y=0, T) = \\ &\frac{1}{(2\pi)^3} \int_{-\infty}^{\infty}\int_{-\infty}^{\infty}\int_{-\infty}^{\infty} S_{\varphi_1}(\boldsymbol{\kappa}, \Omega) e^{-j\Omega T} d\kappa_x d\kappa_y d\Omega \end{aligned} \tag{8}$$

Wherein $S_{\varphi_1}(\boldsymbol{\kappa}, \Omega) = S_{\varphi_1}(\boldsymbol{\kappa})\, \delta(|\Omega| - \kappa_\perp \nu_d)$, $\kappa_\perp$ is the magnitude of the component of the density irregularity wave number perpendicular to the earth's magnetic field. After a similar manipulation in (6), the temporal autocorrelation can be finally determined by (9)

$$\begin{aligned} R_{A_c}(T_c) &= \left\langle e^{-j\varphi_1(x,y,T) + j\varphi_1(x,y,T+T_c)} \right\rangle \\ &\approx 1 - \left\langle \varphi_1^2 \right\rangle \kappa_0^2 v_d^2 T_c^2 / 2 \end{aligned} \tag{9}$$

Where v_d is the plasma drift velocity. T_c indicates the correlation scale in time.

Together with (7), we have addressed the determination of the space-time correlation, which is primarily dependent on the outer scale length of the plasma density irregularities, the plasma drift velocity and the mean square phase fluctuation magnitude. And such intrinsic dependency can also find its verification in our subsequent simulation tests.

2.2. Statistical Distribution Analysis Based on Multiple Phase-Screen Method

Previously, our attention has been captured to measure the space-time correlation of ionosphere perturbed phases. Afterwards, the statistical distribution of which will be discussed.

To this end, we firstly denote $\chi_c(\rho_l)$ as a space-time sampling of signal wavefront at the horizontal scale. Associated with the multiple phase-screen method proposed in [6],[7], the fluctuation process of $\chi_c(\rho_l)$ can be simulated by solving a differential equation above and below these phase subscreens once propagating through the plane stratified ionosphere structure containing irregularities. According to the multiple phase-screen technique, several random phase screens are placed in the ionosphere and therefore the plane stratified ionosphere structure with a thickness of z_t can be divided by M thin phase screen intervals with the size of $\Delta z = z_t/M$. Then the height of the each interval is yielded by $z_i = i \cdot \Delta z \; (i = 0, 1, 2, \cdots, M)$. To proceed, we assume that the horizontal scale of each phase screen is L_h and is divided into L partitions where the random phase changes at $\rho_l = l \cdot \Delta\rho \; (l = -L/2, \cdots, L/2-1)$ can be represented by

$$\psi_i(\rho_l) = \sum_{s=-L/2}^{L/2-1} \sqrt{S_{\varphi_{1_{i-1,i}}}(s\Delta\kappa)\,\Delta\kappa}\,\cos\left(\frac{2\pi l s}{L} + \varphi_s\right) \tag{10}$$

Where $\Delta\rho = L_h/L$, $\Delta\kappa = 2\pi/L_h$, $\varphi_s \in [0, 2\pi]$ is assumed as uniform distribution and the power spectrum for the phase distortions on the screen from z_{i-1} to z_i is given by

$$S_{\varphi_{1_{i-1,i}}}(\kappa_x, \kappa_y, \kappa_z) = \frac{\pi\kappa_e^2}{2}\left[(1-a)^2 z_t \ln\left(\frac{z_t - z_{i-1}}{z_t - z_i}\right) - \frac{z_i^2 - z_{i-1}^2}{2z_t} - (1-2a)\,\Delta z\right] S_{n_1}(\kappa_x, \kappa_y, \kappa_z) \tag{11}$$

In (11), a, κ_e are the modification factor for the case of oblique incidence (cf. (18), (58) in [7]). Combining (10) and (11), the total accrued phase variation of one space-time sampling at each phase screen in the horizontal scale after travelling through the M phase screens can be calculated approximately by the discrete summation instead of continuous integral $\chi_c(\rho_l) = \sum_{i=0}^{M} \psi_i(\rho_l)$. To investigate the statistical distribution of $\chi_c(\rho_l)$, the histogram test will be undertaken in our subsequent simulations.

2.3. Space-time Autocorrelation Simulation and Statistical Distribution Test

Without loss of generality, we restrict our simulations to three scenarios corresponding to different fluctuation states of ionosphere irregularities. The correlation coefficient is assumed as 0.5. And other relevant parameters are recorded in Table 1, where σ_{n_1} is the fluctuation variance indicating the strength of irregular distortions, N_e is the peak ionosphere density, z_b is the distance between the bottom of ionosphere and the ground and θ_e is the angle of incidence.

Table 1. Simulation parameters corresponding to different ionosphere irregular states.

Ionosphere parameters	Case 1	Case 2	Case 3
σ_{n_1}	0.8×10^{-3}	1×10^{-3}	1.2×10^{-3}
$N_e(m^{-3})$	2×10^{11}	4×10^{11}	5×10^{11}
$\theta_e(degree)$	60	50	40
$\nu_d(m/s)$	50	70	100
$z_t(km)$	19	60	120
$z_b(km)$	85	125	200

As illustrated in Fig.1(a)∼(c) (at the top of next page), the spatial correlation distance normally ranges from hundreds of meters to several kilometers with the correlation time of tens of seconds which are largely constrained by the outer scale of irregularity length and operating frequencies. The spatial correlation mainly restricts the azimuth resolving capabilities and hence determines the estimation accuracy of angle of arrival. Such influence can be modelled as the covariance matrix taper (CMT) and has been well studied in [11]. Herein, we mainly focus on the effects on Doppler spectrum qualities imparted by the temporal correlation of ionosphere irregularity. Using the Wiener-Khinchin theorem, this can be guaranteed by a selected power spectrum of the perturbed phases.

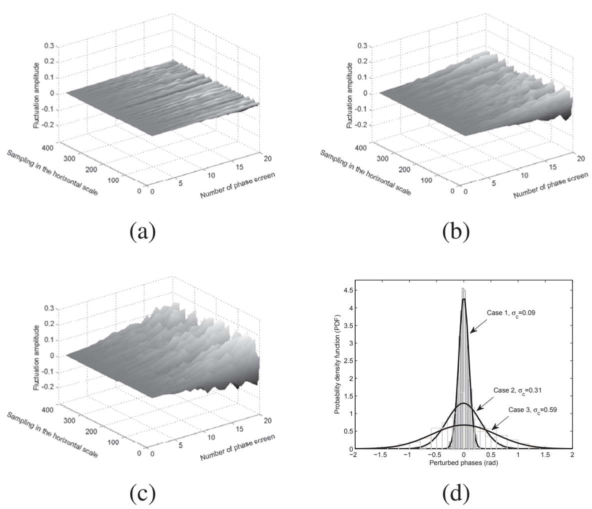

Fig. 2. Illustration of the ionosphere perturbed phases at each phase screen and histogram test results of $\chi_c(\rho_l)$ where $f_0 =$ 12 MHz, $M = 20$ and the outer scale length $L_0 = 2.5km$.

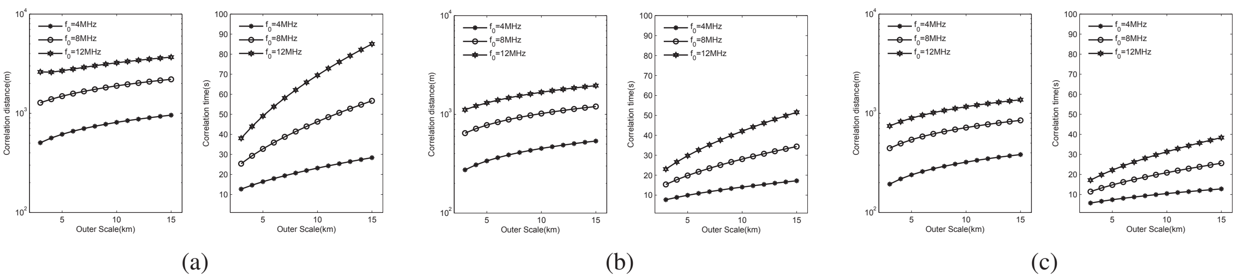

Fig. 1. Correlation characteristics of ionospheric perturbed phases in space and time versus different ionospheric irregular fluctuation conditions.

Commensurately, in concordance with the situations in Table 1, the fluctuation magnitude of the perturbed phases at each subscreen is simulated in Fig.2(a)∼(c). Apparently, the fluctuation strength increases with the incidence depth. In Fig.2(d), histogram tests are carried out to illustrate the distribution of the perturbed phase magnitude. As noted, it follows the Gaussian distribution with a standard variance σ_c ranging from 0.1 to 0.6 corresponding to diverse ionosphere irregular states and the scope of which is generally assumed as the range of phase scintillations from weak to strong.

3. CORRELATION-STATISTICS-BASED SIMULATOR DERIVATION

As alluded to earlier, the power spectrum and statistics of the perturbed phases have been theoretically studied. Associated with the zero memory nonlinear (ZMNL) technique (cf. [12], the principle of which is illustrated in Fig.3.), it is feasible to generate our desired time series by making both subject to some specific distributions. By doing this, the so called correlation-statistics-based simulator is yielded to simulate the perturbed phases triggered by the ionosphere irregularities.

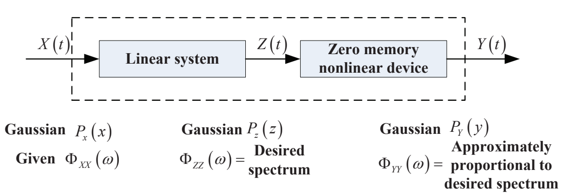

Fig. 3. Principle of ZMNL to generate desired time series.

In Fig.4, the validity of the proposed method is verified through the similar scenarios with Table 1, where the correlation time is restricted to $10s$, $50s$ and $100s$ respectively and the perturbation variance is postulated to be the same as the results in Fig.2(d). In particular, instead of using the theoretical Shkarofsky spectrum [10], the Gaussian power spectrum is considered herein for their similarity as well as the expedience to construct a deterministic relationship between the correlation time T_c and standard variance $\sigma_{0.5}$, where a simple reciprocal relationship between T_c and $\sigma_{0.5}$ is presumed. According to the simulation results illustrated in Fig.4, the simulated ionospheric perturbed phases can agree well with the assumed situations. Obviously, the obtained simulator is capable of producing desirous random time series, obeying the given correlation and statistical distribution independently. And the generation of which would be very helpful in understanding the echo spectral signatures after travelling through the ionosphere non-uniform random medium.

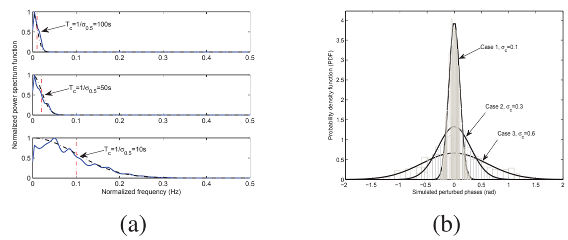

Fig. 4. Effectiveness verification of the proposed method.

4. CONCLUSIONS

In the present paper, the correlation-statistics-based simulator is yielded to generate the perturbed phases triggered by the ionospheric irregularities. The essence of the proposed method is to guarantee the generated time series satisfying specific power spectrum and statistical distribution, which can be realized through the ZMNL technique. Eventually, simulations are carried out to verify the effectiveness of the proposed simulator. Intuitively, the attached perturbed phases involved in the signal echoes scattered back from the ionosphere would largely deteriorate the Doppler spectrum qualities. And a full analysis of which is bound up to facilitate the enhancement of resolving capacities in Doppler for HF radar systems.

5. REFERENCES

[1] K. Lu, X. Liu, and Y. Liu, “Ionospheric decontamination and sea clutter suppression for HF skywave radars,” *IEEE J. Ocean. Eng.*, vol.30, pp.455-462, April 2005.

[2] Y. Li, Y. Wei, R. Xu, and C. Shang, “Simulation analysis and experimentation study on sea clutter spectrum for high-frequency hybrid sky-surface wave propagation mode,” *IET Radar Sonar Navig.*, vol.8, pp.917-930, October 2014.

[3] Y. Zhu, Y. Wei, and Y. Li, “First order sea clutter cross section for HF hybrid sky-surface wave radar,” *Radioengineering*, vol.23, pp.1180-1191, December 2014.

[4] C.J. Coleman, “A model of HF sky wave radar clutter,” *Radio Sci.*, vol.31, pp.869-875, July-August 1996.

[5] K.C. Yeh, and C.H. Liu, *Theory of ionospheric waves*, Burlington, MA: Elsevier, 1972, pp.231-234.

[6] Y. W. Kiang, and C. H. Liu, “Multiple phase-screen simulation of HF wave propagation in the turbulent stratified ionosphere,” *Radio Sci.*, vol.20, pp.652-668, May-June 1985.

[7] J.F. Wagen and K.C. Yeh, “A numerical study of waves reflected from a turbulent ionosphere,” *Radio Sci.*, vol.21, pp.583-604, July-August 1986.

[8] S.M. Rytov, Y.A. Kravtsov, and V.I. Tatarskii,“Wave propagation through random media,” in *Principles of statistical radiophysics*, Berlin: Springer, 1989.

[9] M. Ravan, R.J. Riddolls, and R.S. Adve, “Ionospheric and auroral clutter models for HF surface wave and over-the-horizon radar systems,” *Radio Sci.*, vol.47, pp.1-12, June 2012.

[10] I. P. Shkarofsky, “Generalized turbulence space-correlation and wave-number spectrum-function pairs,” *Can. J. Phys.*, vol.46, pp.2133-2153, June 1968.

[11] R.J. Riddolls, “Detection of aircraft by high frequency sky wave radar under auroral clutter-limited conditions,” Ottawa, ON, Tech. Rep. TM 2008-336, March 2009.

[12] R.L. Mitchell, “Generating random sequences,” in *Radar Signal Simulation*, Washington: Artech House, 1976, pp.111-127.